Chapter 3

MODELS OF THE OCEAN: WHICH OCEAN?

Anne Marie Treguier
CNRS, LPO, Plouzané, France

Abstract Physics actually represented in an ocean model depend on each model's resolution and its parameterization of subgridscale effects. This chapter is a review of parameterizations used in ocean models, focussing on operational ocean forecasting systems for the North Atlantic and Mediterranean Sea. This review is limited to z-coordinate models. A detailed presentation of the physics underlying each parameterization is out of the scope of this short chapter, but we try to discuss some uncertainties of the physical basis of current parameterizations. The concept of subgrid scale effects and some interesting properties of the diffusion equation are presented first. Because ocean turbulence is strongly anisotropic, parameterization in the vertical and horizontal (or isopycnal) directions differ and are presented separately. Special sections are devoted to bottom boundary layers, flow topography interactions, and the dynamical effects of mesoscale eddies.

Keywords: Parameterizations, ocean modelling, numerical models, subgrid scale physics, diffusion, viscosity.

A simplistic view of the surface ocean circulation is often found in geographical maps, with arrows displaying the direction and location of the main surface currents. Those are the large scale, wind driven currents which Sverdrup and Stommel, among others pioneers, have tried to understand. The first models of the wind-forced ocean circulation that they built were two-dimensional, used the simplified quasi-geostrophic equations, and the western boundary currents were viscous boundary layers.

This linear, viscous ocean is still what is represented in most climate models today. The sea surface height distribution in the South Atlantic

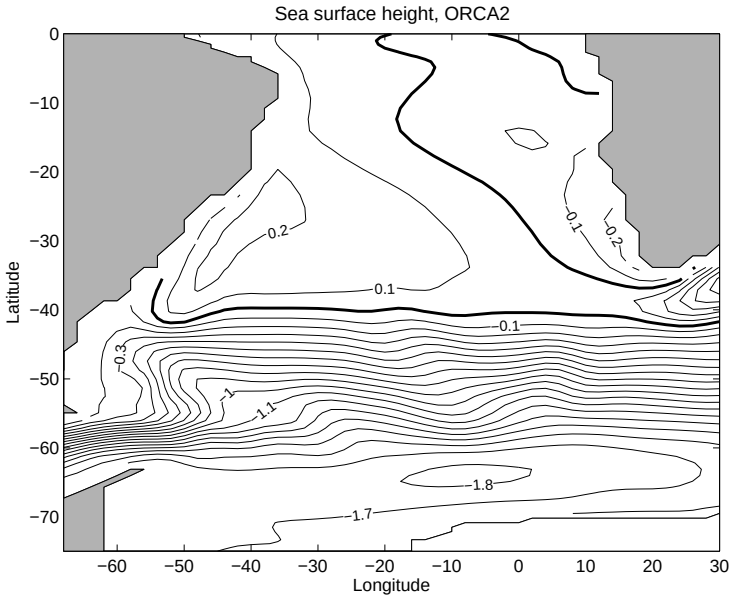

Figure 1. Sea surface height (ssh) in the south Atlantic in the global ORCA2 model (G. Madec). The ssh is averaged over one year, at the end of a 100 year experiment. Contour interval is 0.1 m, the zero contour is indicated in dark.

from the global 2° model ORCA2 (Fig. 1) is completely in agreement with the image of the ocean conveyed by simplified maps. Of course, the climate models are three dimensional, so that they are able to represent the global overturning circulation. In fact, the latter is often represented by a diagram of the "conveyor belt", similar to the sketchy geographical maps of surface currents.

Observations show that the real ocean is turbulent over a wide spectrum of spatial and temporal scales, and non-viscous. Today high resolution models begin to represent realistically the ocean we observe, and provide pictures in stark contrast with Fig. 1. One example is the POP 1/10° global model represented in Fig. 2 (Maltrud and McClean, 2004).

ORCA2 and POP 1/10 are so different that one may argue they do not represent the same ocean. A similar contrast exists between the ATL1 and ATL6 models of the CLIPPER group (Treguier et al., 2001). ATL1 and ATL6 are Atlantic models with 1° and 1/6° spatial resolution, respectively. Fig. 3 represents float trajectories during 5 years in the deep western boundary current of the South Atlantic, at 1800m. The coarse resolution ATL1 model depicts a sluggish western boundary current, with a well-defined southward velocity. Most of the floats reach

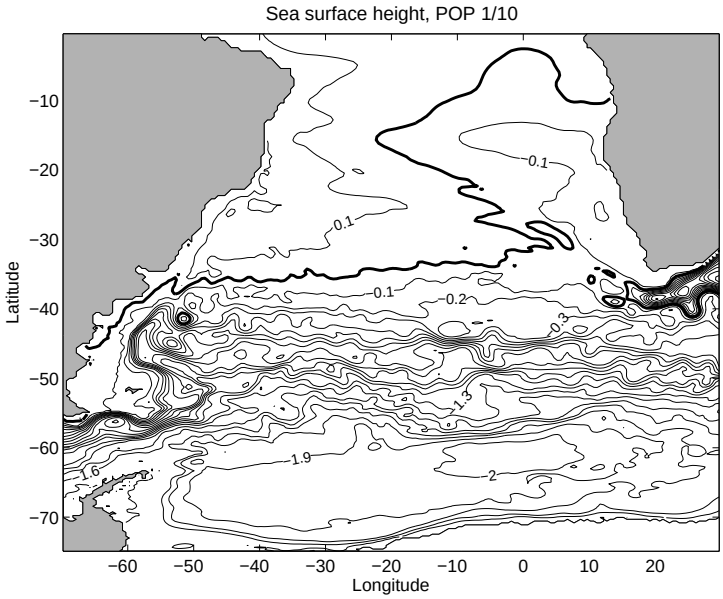

Figure 2. Sea surface height (ssh) in the south Atlantic in the global POP 1/10° model. The ssh is averaged over one year (fifth year of the experiment). Contour interval is 0.1 m, the zero contour is indicated in dark.

30°S after 5 years. In the ATL6 model, some trajectories go north instead of south because the western boundary current at that latitude often breaks down in a series of eddies (this has recently been observed by Dengler et al. (2004). Only one ATL6 float goes farther south than 30°S, but it gets there faster than the ATL1 floats, and many ATL6 floats escape into the interior of the ocean: this behavior is illustrative of chaotic mixing. The flow of the deep water in models like ATL1 is consistent with our simplified picture of the "conveyor belt"; high resolution models like ATL6 provide a picture much more difficult to interpret. They are closer to the real ocean, and yet too far from it to give us confidence in quantitative estimates. For example, the eddy kinetic energy at 2400m near 34°W, 22°S is 7.1 cm^2s^{-2} in ATL6 while a value of 62.1 cm^2s^{-2} has been measured there (Treguier et al., 2001). Underestimation of eddy kinetic energy at depths is very common in ocean models (Penduff et al., 2002).

It is important to realize that ATL1 and ATL6 are the same model, from the numerical and computational point of view. Both solve the same primitive equations, with the same code (OPA8.1, Madec et al. 1998). However, they are not models of the "same ocean", because they

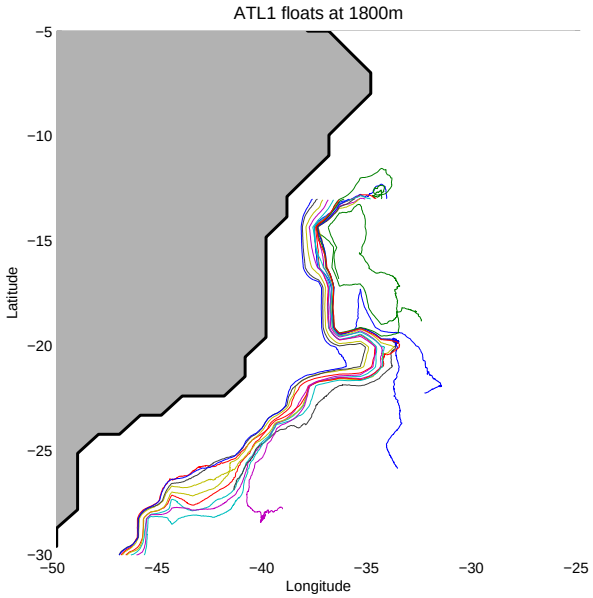

Figure 3. Trajectories of 15 numerical floats seeded at 1800 m, at 13°S every 1/4° from 37.75°W to 34.25°W. The trajectories are integrated during 5 years in the ATL1 1° model.

do not use the same parameterizations. In choosing the resolved spatial and temporal scale, and the parameterizations of the subgrid scales, the modeller effectively chooses the ocean he (or she) wishes to model. The present chapter discusses these choices.

When setting up an ocean model configuration, we have to ask ourselves which parameterizations are the most suitable, which coefficients to use for those parameterizations, and how changes in those coefficients would affect our solutions. We can answer surprisingly few of those questions for realistic ocean models, due to the complex interaction between different parameterizations (not to mention the interplay between physical parameterizations and numerical schemes). This is especially true for eddy permitting models for which extensive parameterization studies are not yet feasible due to the computational cost and the long time scales involved.

This chapter includes a discussion of sub-grid scale effects and general properties of the diffusion equation (part 2), and a discussion about parameterizations used in ocean models (parts 3 to 6). The parameterization issue has recently been the subject of a whole set of courses (Chassignet and Verron, 1998) It is discussed in the context of climate models in a paper by Griffies et al. (2000a), and also in Griffies' book

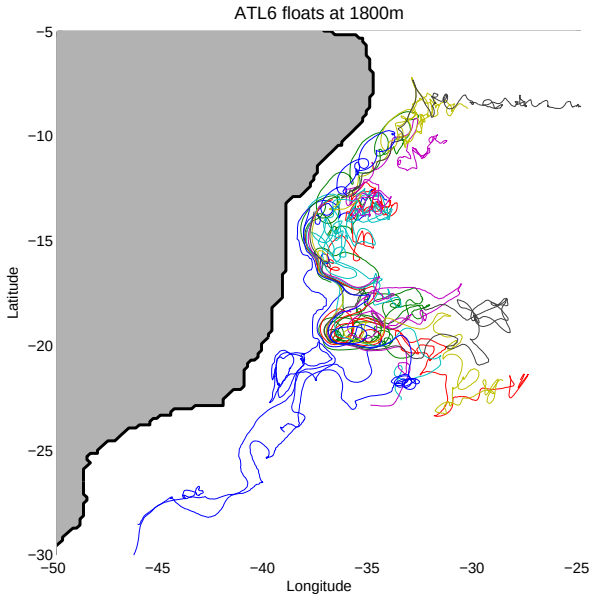

Figure 4. Same as Fig. 3, for the ATL6 1/6° model.

(Griffies, 2004) where the relationship between numerical schemes and parameterizations is analyzed in depth. In this short course I will survey parameterizations, hopefully providing a useful (albeit superficial) introduction to the more exhaustive material. Focus is on current practice, with little discussion of the underlying physical processes. The interested reader is referred to Chassignet and Verron (1998), or references therein.

1. Sub-grid scale effects in ocean models

1.1 Convergence of numerical solutions

We can write the prognostic equations of an ocean model in the general form:

$$\frac{\partial \mathbf{Y}}{\partial t} + \mathbf{V}.\nabla\mathbf{Y} + F(\mathbf{Y}) = 0 \tag{1}$$

where $\mathbf{Y} = (\mathbf{V}, T, S)$ is the vector of prognostic variables with $\mathbf{V}$ the velocity vector, T the potential temperature, S the salinity. The second term is nonlinear advection and the third term F represent all other terms, including external forcings. The equations must be discretized in order to be solved numerically: in ocean models this is usually done by choosing a mesh of grid points and using finite difference formulae.

The model solves for $\mathbf{Y_R}$ which is the resolved state of the ocean, on spatial scales of a grid cell, at discrete times. Using the terminology of Boer and Denis (1997), $\mathbf{Y_R}$ results from applying a "numeric resolution" operator $()_R$ to the state vector $\mathbf{Y}$. The definition of the "resolved" scales involves some kind of averaging: appropriate averaging operators for ocean dynamics are discussed extensively by Griffies (2004). Let us apply the operator $()_R$ to (1):

$$\begin{aligned} \frac{\partial \mathbf{Y_R}}{\partial t} &+ \mathbf{V_R}.\nabla \mathbf{Y_R} + F_R(\mathbf{Y_R}) = \\ &- ((\mathbf{V}.\nabla \mathbf{Y})_R - \mathbf{V_R}.\nabla \mathbf{Y_R}) - (F(\mathbf{Y})_R - F_R(\mathbf{Y}_R)) \,. \end{aligned} \quad (2)$$

We have to account for the effect of unresolved scales on the evolution of $\mathbf{Y_R}$ (the right hand side of (2)). When this effect is not represented correctly we make a *parameterization error*, which is different from the *numerical error* made by using a finite difference approximation in solving the left hand side of (2). Note that the advective contribution to subgrid scale effects (first term on the right hand side of (2)) does not vanish even in an inviscid fluid. This happens because turbulent motions usually generate a cascade of variance of the resolved quantity towards small scales (say, for a tracer, as discussed for example in Dubos and Babiano (2002). It is necessary for the parameterization to dissipate tracer variance to represent this cascade in the limited spectral space of a numerical model, even when the physical processes involved are related to stirring rather than mixing.

¿From a mathematical point of view, one would like to see the solution of an ocean model to converge as the resolution is increased (that is, progressive refinements of the resolution should bring smaller and smaller changes in the solution). However, when we refine the grid (as between Fig. 1 and Fig. 2) we also change the parameterizations on the right hand side, and thus we solve different equations. The huge differences in the solutions of ORCA2 and POP 1/10 do not come from a faulty numerical scheme; rather they come from the fact that the parameterizations differ. Let us note, however, that even the numerical (mathematical) convergence of z coordinates model solutions is not demonstrated, and indeed there are examples of non-convergence (Gerdes, 1993) due to the staircase representation of the topography.

Taking a physical point of view, convergence can be expected only over a range of scales where the dynamics of the flow remains qualitatively the same, so that the same parameterizations can be consistently applied. Atmospheric scientists have been able to set up test problems to look for the convergence of the dynamical core of their climate models (allowing representation of synoptic scale turbulence). Boer and Denis

(1997) present such a setting: an aquaplanet (no topography), a dry atmosphere, with a large scale forcing including prescribed heating and weak relaxation to a temperature profile. In the ocean it is much more difficult to find test problems that are relevant to climate. Two similar problems have been submitted to a convergence test. The first one is the flat-bottom, quasigeostrophic basin, relevant to the study of the upper ocean wind forced response (Siegel et al., 2001). The domain had a width of 3500 km with six layers in the vertical; the smallest dynamical spatial scale, the sixth internal Rossby radius, was close to 10 km. The second test case is a layered model of the North Atlantic (Hurlburt and Hogan, 2000) with 6 layers in the vertical, realistic coastline and topography restricted to the bottom layer. In both studies the authors still found significant differences between horizontal resolutions of 3 and 1.5 km (1/32°and 1/64°), either in energy and potential vorticity fluxes or in local aspects of the circulation. However, the differences were smaller than between lower resolution cases (say, between 1/8°and 1/16°), suggesting that the highest resolution cases approached convergence.

It is possible to relate the oceanic case to the atmospheric case considering the different dynamical scales (Rossby radii) in the two fluids. Boer and Denis (1997) consider in their test case that the dynamics have converged at T63, that is, a resolution of 1.87° (about 150 km at mid latitudes). This is 18% of the first internal Rossby radius R_o which is about 800 km in the atmosphere. An equivalent resolution in the ocean would be 7 km in the subtropics ($R_o = 40$ km) and 2 km in subpolar regions ($R_o = 12$ km). Those results suggest that none of today's basin scale models can be called "eddy resolving" in the subpolar regions, and that parameterizations should take into account the part of the mesoscale spectrum that is not resolved.

1.2 Subgrid scale turbulence

The first subgrid scale effects that usually come to mind are those related to the nonlinear advection terms, that is, the first term on the rhs of (2). To develop parameterizations one further assumes that

$$(V.\nabla \mathbf{Y})_R - V_R.\nabla \mathbf{Y_R} = (V'.\nabla \mathbf{Y}')_R, \tag{3}$$

where $\mathbf{Y}' = \mathbf{Y} - \mathbf{Y_R}$ is the subgrid scale part of $\mathbf{Y}$. This is true only if the "resolution operator" has the properties of a Reynolds average, which is not the case for a spatial truncation (among other properties, a Reynolds average commutes with spatial and temporal derivatives, and the average of the deviation $\mathbf{Y}'$ is zero). Assuming a Reynolds decomposition (for lack of something more accurate) the subgrid scale effects appear as the divergence of eddy fluxes. Equations can be written for

those eddy fluxes, such as the Turbulent Kinetic Energy (TKE) equation. They involve higher order moments of the turbulent variables so that a "closure hypothesis" is required to solve them: this consists in using an empirical relationship to express higher moments in term of the lower-order moments. A classical example of closure model for vertical mixing in the ocean is provided by Mellor and Yamada (1982). The simplest closure applies to the advection of a passive tracer by homogeneous and isotropic turbulence. Eddy fluxes in that case can be modelled by analogy with the molecular diffusivity (Fickian hypothesis): for example

$$(w'T')_R = -\kappa \frac{\partial T_R}{\partial z}. \tag{4}$$

The vertical eddy temperature flux is down the gradient of resolved temperature.

It is usually assumed that the ocean turbulence is isotropic at the centimeter scale, so this simple parameterization would apply. At larger scales, the physical processes that one needs to parameterize are more complex and no longer isotropic. The first ingredients that break isotropy are the effects of gravity and stratification. Stratified fluid supports internal waves, which can carry energy far from their generation site; stratification inhibits cross-isopycnal motion and cross-isopycnal mixing. Furthermore, when it is unstable, stratification generates convective instabilities. These must be parameterized regardless of the grid scale and time step of the model when the hydrostatic approximation is made (it is the case in primitive equation models). An additional physical process in the ocean is the double diffusive convection arising from the different molecular diffusivities of heat and salt. Going to larger scales, the earth rotation comes into play (time scale of one day, horizontal scale of hundreds of meters). It creates the possibility of resonant inertial motions, and further inhibits vertical motion. Finally, at the mesoscale, the variation of the Coriolis parameter with latitude is important. The vanishing of the Coriolis force at the equator makes it a waveguide and allows inertial instability. The β effect at mid latitudes tends to favor zonal motions and inhibit meridional mixing. All those physical processes are reviewed in detail in the book edited by Chassignet and Verron (1998).

In three dimensions, a linear relationship as (4) between local eddy fluxes and local mean gradient components can be expressed as the product of the gradient vector by a matrix:

$$(v_i'T')_R = -T_{ij} \frac{\partial T_R}{\partial x_j}, \tag{5}$$

where v_i are the velocity components and T_{ij} is the mixing tensor. Mathematically, the tensor can be decomposed as the sum of a symmetric part

K_{ij} and an antisymmetric S_{ij} part. With classical isotropic diffusion, K_{ij} is diagonal with mixing coefficient κ along the diagonal, and S_{ij} is zero. Taking into account the anisotropy of ocean motions requires a different coefficient for horizontal and vertical mixing. More generally, the symmetric tensor K_{ij} can be diagonalized along principal mixing directions; in the ocean those are assumed to be along and across isopycnal (isoneutral) directions respectively (see section 5.2). The corresponding paramerization in the temperature and salinity equations for an ocean model is called "isopycnal laplacian diffusion", by contrast with horizontal diffusion.

One way to understand the antisymmetric part S_{ij} is the following. With eddy fluxes defined by (5) the equation for the resolved temperature T_R includes the divergence of the eddy fluxes, with a contribution from the antisymmetric tensor written as:

$$\nabla(-S_{ij}\frac{\partial T_R}{\partial x_j}). \tag{6}$$

It is easily demonstrated that this term is identical to an advection of T_R by a velocity V^* with components defined by:

$$v_i^* = \frac{\partial S_{ij}}{\partial x_j}. \tag{7}$$

As a consequense, in our idealized framework of a linear relationship between eddy fluxes and mean gradients, parameterizations can be classified in three components: the vertical (cross isopycnal) and the lateral (isopycnal) mixing associated with the symmetric tensor K_{ij}, and the advective eddy effect associated with S_{ij}. Those three components will be considered in turn in sections 3, 5 and 6 of this chapter. The interested reader will find a complete discussion of the mixing tensor (as well as an alternative presentation using the notion of skew flux) in Griffies (2004).

1.3 The diffusion equation

Parameterizations often assume a flux gradient relationship like (4), and look like a diffusion. It is important to realize that the diffusion equation has some unexpected properties when the mixing coefficient is allowed to vary. Let us consider for example the evolution of a vertical profile of potential temperature, when the vertical eddy flux is parameterized by (4). The initial temperature perturbation T is sinusoidal over a depth H and evolves according to the equation:

$$\frac{\partial T}{\partial t} = \frac{\partial}{\partial z}\left(\kappa\frac{\partial T}{\partial z}\right) = \kappa\frac{\partial^2 T}{\partial z^2} + \frac{\partial \kappa}{\partial z}\frac{\partial T}{\partial z}. \tag{8}$$

With constant κ this is a classical diffusion equation and the perturbation decays with a characteristic time $\tau = H^2/(\pi^2\kappa)$.

When κ varies vertically, the second term on the right-hand side of (8) is non zero. It is similar to a vertical advection with velocity

$$w_\kappa = -\partial\kappa/\partial z.$$

This term can lead to a sharpening of the large scale gradients (P. Klein, personal communication). To see this, let us consider the equation for the temperature gradient T_z, obtained by taking the vertical derivative of (8):

$$\frac{\partial T_z}{\partial t} = \kappa\frac{\partial^2 T_z}{\partial z^2} + 2\frac{\partial\kappa}{\partial z}\frac{\partial T_z}{\partial z} + \frac{\partial^2\kappa}{\partial z^2}T_z. \tag{9}$$

The first term is the diffusion, the second the advective contribution, and the third term can cause an exponential growth of the temperature gradient when $\partial^2\kappa/\partial z^2$ is large enough. This happens if κ varies more rapidly in space than T. Let us assume, for instance, that the initial T profile has some small scale variations superimposed on it, and that the physical processes generating mixing are very sensitive to the presence of those small scales. This situation is displayed in Fig. 5. The mixing cofficient has large values where the small scales are present, in the upper third part of the water column. Instead of decaying, the profile of temperature after 120 days has a much stronger gradient. The T profile, initially of typical scale H, varies now with the typical spatial scale of the κ profile. The temperature perturbation has also been advected downwards. Note that although a sharpening of the gradient has occurred, diffusion has smoothed the local extrema in the initial profile as expected (this property of the diffusion equation is independent of the structure of the diffusion coefficient).

Even more interesting things happen when κ is a nonlinear decreasing function of $\partial T/\partial z$. When κ is nonlinear enough, the parameterization can generate discontinuities and staircases in the temperature profile. Fig. 6 shows the final state of the evolution of eq.(8) with κ proportional to $\exp(-(dT/dz)^2)$. This effect was noted by Phillips (1972) and more recently by Ruddick et al. (1989)

Letting κ be a decreasing function of the vertical temperature gradient is precisely what parametrizations of vertical mixing do: stratification inhibit vertical mixing by providing a strong restoring force (buoyancy force), thus limiting vertical displacements. Most parameterizations of vertical mixing are based on the Richardson number of the large scale flow. Let us define first the Vaisala frequency N:

$$N^2 = \frac{-g\partial\rho/\partial z}{\rho_0},$$

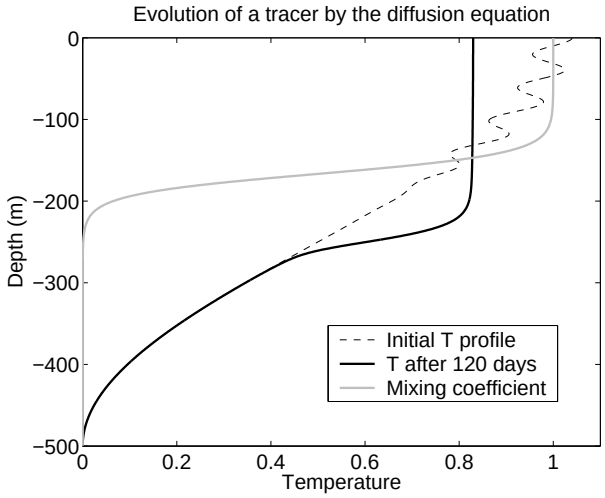

Figure 5. Initial and final solution of the diffusion of a tracer according to (8) with no flux boundary conditions, when $\kappa = 0.005 \tanh(\alpha(z - H/3)) + 1)$ $\mathrm{m}^2.\mathrm{s}^{-1}$, with $H = 500$ m and $\alpha = (0.05H)^{-1}$. The profile of the mixing coefficient κ is multiplied by 100 to be displayed on the same scale as T.

where ρ is density and g gravity. The Richardson number is:

$$Ri = \frac{N^2}{(\partial u/\partial z)^2 + (\partial v/\partial z)^2},$$

with u and v the horizontal components of velocity. This dimensionless number expresses the competition between the stabilizing effect of stratification and the destabilizing effect of the shear. Parameterizations of vertical mixing always produce mixing coefficients that are strongly nonlinear functions of the Richardson number, displaying an almost "step-like" behavior with strong mixing at low Richardson numbers and little mixing for Richardson numbers above critical (see for example fig 23 of Blanke and Delecluse, 1993, or Fig. 5 of Large, 1998). This behavior is sound physically and is observed in the ocean, but may create numerical problems. Modellers need to be aware of the profound implications of spatially variable mixing coefficients.

1.4 Subgrid scale effects of external forcings and boundary conditions

Besides the nonlinear interactions inside the fluid itself, external forcings also generate subgrid scale effects: it is the case for ocean-atmosphere interactions. For example, heat fluxes and evaporation depend on the

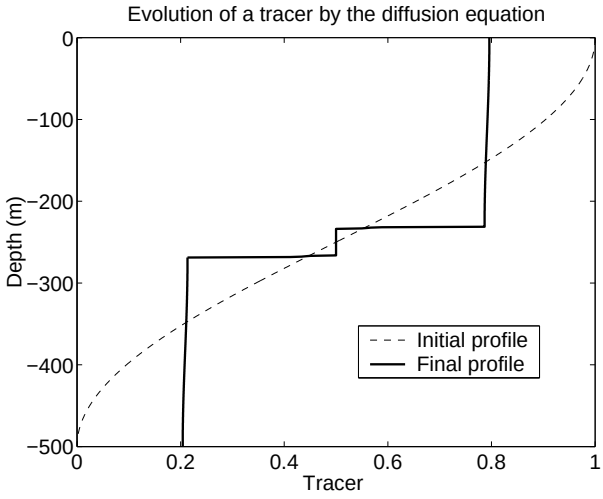

Figure 6. Initial and final solution of the diffusion of a tracer according to (8) with no flux boundary conditions, when $\kappa = 0.01 \exp(-(0.59 H dT/dz)^2)$, with $H = 500$ m.

sea surface temperature, and can be very different above mesoscale eddies. Arhan et al. (1999) estimate an average heat loss of 620 W.m^{-2} above an Agulhas eddy in 6 months, much higher than climatological values in the area. No attempts have been made yet to parameterize this effect in climate models where eddies are absent. In eddy resolving ocean models, subgrid scale effects arise because of the low resolution of the forcing fields or the atmospheric models used for coupling. The mesoscale response of the atmosphere to SST perturbations is ignored in such models. Finally, according to the temporal resolution of the forcing fields, there may be non-resolved time scales as well: for exemple the effect of wind bursts, or the diurnal cycle of radiative forcing. These sub-grid scale effects will not be discussed further here but should be kept in mind.

Perhaps the most important and complex sub-grid scale effect arises through the boundary conditions, namely the shape of the ocean basins. The first example is the communication between ocean basins and semi-enclosed seas: according to the spatial resolution of the model, it is possible or not to represent some straits. Some aspects of the parameterizations of subgrid scale topography are presented in section 4.

2. Parameterizations in the vertical

After introducing sub-gridscale effects, let us now review parameterizations, considering in turn the vertical direction (this section), bottom

Parameters	PSY2	FOAM	MFS-MOM	MFS-OPA
Code	OPA	MOM	MOM	OPA
Time step	δt = 800s	δt =1200s	δt =900s	δt =600s
Domain	N. Atlantic+Med	N. Atlantic	Mediterranean	
Horizontal grid:				
Max δx	7 km	12 km	12 km	6 km
Min δx	3 km	12 km	9.8 km	4.9 km
Vertical grid:				
levels	43	20	31	72
Max δz	300 m	615 m	300 m	300 m
Min δz	6 m	10 m	10 m	3 m
Lateral boundary condition:	partial-slip	no-slip	no-slip	no-slip

Table 1. Grid and domain for four z-coordinate models used in forecasting systems: PSY2 (MERCATOR, France), FOAM (U.K. Met Office) and two MFS systems (Italy)

and topographic effects (section 4), mixing laterally or along isopycnals (section 5) and dynamical effects of mesoscale eddies (section 6). Because this book is about operational oceanography, I will consider as examples three z-coordinates ocean models that are currently part of an operational forecasting system (table 1).

The parameterizations used in those models are listed in table 2. Three of the models, PSY2, MFS-OPA and MFS-MOM have quite similar, rather simple parameterizations. FOAM has more complex parameterizations, mainly because this eddy permitting model has been derived from a lower resolution climate model (Gordon et al., 2000). It would be interesting to know the impact that those more elaborate parameterizations have on the results of the forecasting system.

In this section we discuss the parameterization of processes that cause vertical mixing in the surface boundary layer or in the interior: convective mixing, shear instabilities, inertial waves breaking, double diffusion. It is important to note that the parameterizations of those processes are often lumped together in one package. This is the case of the "KPP" parameterization (Large et al., 1994). Its originality lies in the parameterization of the surface mixed layer, using a prescribed vertical profile of fluxes adjusted on a mixed layer depth (K-profile), but Large et al. (1994) also propose a parameterization of convection, interior and double diffusive mixing. This is why the parametrizations for vertical diffusivity and viscosity in the interior and in the upper mixed layer are lumped together in table 2.

	PSY2	FOAM	MFS-MOM	MFS-OPA
Vertical diffusivity				
Background	1. 10^{-5}m^{2}s^{-1}		3. 10^{-5}m^{2}s^{-1}	3. 10^{-5}m^{2}s^{-1}
Ri dependent	TKE	PP81	none	none
Other	Surf.E	KPP+KT67	none	none
Vertical viscosity				
Background	1. 10^{-4}m^{2}s^{-1}		1.5 10^{-4}m^{2}s^{-1}	1.5 10^{-4}m^{2}s^{-1}
Ri dependent	TKE	PP81	none	none
Other	Surf.E	KPP+KT67		
Convection				
Adjustment	no	yes	yes	no
Enhanced mixing	1 m^{2}s^{-1}			1 m^{2}s^{-1}
Lateral diffusivity				
Hor. Biharmonic	3 10^9m^{4}s^{-1}	none	1.5 10^{10}m^{4}s^{-1}	3 10^9m^{4}s^{-1}
Spatial variation	$\propto \delta x^3$		Constant	Constant
Laplacian	none	100 m^2.s^{-1}	none	none
Orientation	hor	iso	hor	hor
slope limitation	no	GE91	no	no
Horizontal background	no	10 m^2.s^{-1}	no	no
Lateral viscosity				
Biharmonic	9 10^9m^{4}s^{-1}	2.6 10^9m^{4}s^{-1}	5 10^9m^{4}s^{-1}	5 10^9m^{4}s^{-1}
Laplacian	none	30 m^2.s^{-1}	none	none
Spatial variation	$\propto \delta x^3$	no	no	no
Bottom friction				
Type	Quadratic	Quadratic	none	quadratic
Coefficient	C_d =1.3 10^{-3}	C_d =1.225 10^{-3}		C_d =10^{-3}
Bottom boundary layer				
Type	none	GO00	none	none

Table 2. Parameterizations for four z-coordinate models used in forecasting systems. Schemes are TKE (Blanke and Delecluse, 1993), PP81 (Pacanowski and Philander, 1981), KPP Large et al., 1994, KT67 (Kraus and Turner, 1967). Note that in FOAM KPP is a modified version (Gordon et al., 2000). Surf.E is an enhancement of background coefficients near the surface. The orientation is either horizontal (hor) or iso-neutral (iso). Note that locally, neutral and isopycnal directions are identical. In the case of isopycnal mixing, modellers have to modify the algorithm whe slopes are too steep. In FOAM this is done using the scheme GE91 of Gerdes (1993). The Bottom boundary layer (GO00) used in FOAM is documented in Gordon et al. (2000).

2.1 Local and non-local parameterizations

As reviewed in detail by Large (1998) parameterizations can be classified into local and nonloncal. Local parameterizations following (4) assume that the eddy fluxes depend on the *local* properties of the large scale flow. They are often based on one-dimensional turbulence closure models, like the TKE model of Blanke and Delecluse (1993). The one-dimensional "stand-alone" models are implemented with grid spacing of order one meter in the vertical; it is unclear how they perform with the typical grid spacing of ocean models (5-10 m at the surface, quickly increasing to 20-50 m at 100 m depth). It is important to keep in mind that the classical Ekman layer depth is $h_e = \sqrt{2\nu/f}$. At mid latitudes, the vertical viscosity ν has to be larger than 5. $10^{-3}\mathrm{m}^2.\mathrm{s}^{-1}$ for h_e to be larger than 10 m (that is, for the Ekman depth to be larger than the first model layer thickness). In the absence of high frequency forcing, in the absence of night time convection, and with low vertical resolutions, turbulent closures cannot produce high enough mixing at the top layer interface. This explains why non-local parameterizations are attractive, like the old Kraus-Turner (Krauss and Turner, 1967) parameterization and the new KPP scheme (Large et al., 1994) used in the FOAM model (Table 2). This is also the rationale for "ad-hoc" fixes like the increase of the background coefficient in the upper layers found in the PSY2 model.

The present versions of the MFS models do not use any parameterization of the surface mixed layer (table 2). In that case, convection is the only source of enhanced mixing. Convection driven by surface cooling allows to reach realistic mixed layer depths in winter in the Mediterranean sea (see Crosnier and Le Provost in this volume). In summer, a shallow convection is driven by the penetration of incoming short wave radiation which warms the water down to a depth of about 15 m, while the outgoing longwave radiation cools the top layer only. Without penetrative solar radiation the mixed layer depth in MFS in summer would be restricted to the first model layer.

The performance of different vertical mixing schemes in realistic ocean models is not well documented, so that it is very difficult to make an objective choice among the different parameterizations. The use of KPP instead of crude parameterizations, like an imposed uniform mixed layer depth, clearly brings an improvement (Large, 1998). An improvement was also found by Blanke and Delecluse (1993) when using TKE instead of the Richardson-dependent scheme of Pacanowski and Philander (1981). On the other hand, a recent comparison of KPP with the TKE scheme (Chanut and Molines, 2004) shows little difference in the 1° CLIPPER Atlantic model. What makes the picture even fuzzier is

the fact that changing tunable constants within one parameterization package has significant effects (Matteoli, 2003). This lack of thorough sensitivity studies, especially for eddy permitting models, will stand out as we discuss the different processes leading to vertical mixing.

2.2 Convection

Early primitive equation models (Cox, 1984) represented convection by an iterative adjustment, which modified temperature and salinity in a water column. Adjustment schemes have convergence problems in some cases and tend to be costly; moreover the time scale of adjustment is one time step, which is too short in high resolution configurations. Despite these shortcomings, they are still in use in some forecasting models (Table 2).

Nowadays convective adjustment is more frequently represented by increasing the vertical mixing coefficient to a very large value in the case of convection. This procedure has been found to be a satisfactory parameterization of the effect of convective plumes by Klinger et al. (1996), with a mixing coefficient of 10 $m^2.s^{-1}$. Scalings suggest values up to 50 $m^2.s^{-1}$ (Send and Käse, 1998). The PSY2 model uses a coefficient of 1 $m^2.s^{-1}$ (table 2); the ORCA2 model uses 100 $m^2.s^{-1}$. Users of the KPP scheme take values from 0.1 to 10 $m^2.s^{-1}$.

The criterion for the onset of convection varies among models; convection is active as soon as the Vaisala frequency N^2 is negative in some models (PSY2) while the criterion in KPP is $N^2 < -0.2\ 10^{-4} s^{-2}$. The relative mixing of momentum and tracers also varies between models. Momentum should be mixed like tracers in convective plumes if the time scale t_{mix} for a parcel to move down the plume is shorter than the $1/f$, the time for geostrophic adjustment. With plume vertical velocities w of order 3 to 10 cm/s (Klinger et al., 1996), $t_{mix} = h/w$ reaches 12 h for deep convection, thus comparable to $1/f$. Tests performed with the ORCA2 model (Matteoli, 2003) show important differences in mean surface velocities (up to 10 $cm.s^{-1}$) in the Antarctic circumpolar current, with and without momentum mixing in the case of convection.

2.3 Interior mixing

As emphasized in the review by J. Toole (Toole, 1998), observations have shown increased levels of mixing in the abyss and over rough topography, compared with the low values found in the thermocline by microstructure measurements and tracer releases. More recently, the role of internal tides as an energy source for mixing has been empha-

sized. Maps of energy flux have been derived from tidal models leading to parameterizations of vertical mixing (Laurent et al., 2002)

Spatially variable vertical mixing coefficients based on topographic roughness or tidal mixing have yet to be tested extensively in models. Studies by Hasumi and Suginohara (1999) and Simmons et al. (2004) show modest improvements in coarse resolution models integrated to equilibrium. The effect of such parameterizations over shorter time scales in higher resolution models needs to be assessed, since uniform mixing coefficients are clearly not acceptable based on the observations.

One has to be aware that z coordinate models have difficulty achieving the vertical mixing coefficients of order $10^{-5}\mathrm{m}^2.\mathrm{s}^{-1}$ in the thermocline, depending on their advections scheme (Griffies et al., 2000b). Since the last decade modellers tend to abandon centered advection schemes, which lead to the generation of unphysical temperatures and salinities near fronts (note, for example, that the ATL6 model of Fig. 4 has one grid point with temperatures lower than -3°C at the bottom of the Faroe Bank channel outflow; salinities close to 42 PSU are found downstream of Gibraltar in the 1/10° model of Smith et al., 2000). Diffusive schemes like FCT (Flux Corrected Transport) avoid such problems, but in eddy permitting z-models they can cause a large amount of diapycnal mixing (Griffies et al., 2000b). The same is true for non-eddy resolving models when the western boundary current is marginally resolved: Griffies et al. (2000b) find spurious diapycnal mixing of 3 $10^{-4}\mathrm{m}^2.\mathrm{s}^{-1}$ due to the advection scheme in that case.

2.4 Double diffusive mixing

Double diffusion occurs in stably stratified situations, either when warm and salty water overlies cold, fresh water (salt fingering) or when cold, fresh water overlies warm and salty water (diffusive convection). Those processes generate turbulent mixing of heat and salt with different coefficients, dependent on the density ratio $R_\rho = \alpha\partial_z T/\beta\partial_z S$, where α and β are coefficients of thermal expansion and saline contraction. A parameterization has been proposed by Large et al. (1994) but it has not been thoroughly tested. A slightly different one has been proposed by Merryfield et al. (1999) and tested in a coarse resolution model, showing and improvement in the representation of water mass temperature and salinity although the effect on the circulation was small. None of the forecasting models listed in Table 2 uses a parameterization for double diffusion, even though this dynamical process is important in the ocean (Schmitt, 1998). A better and cleaner representation of "background" interior vertical mixing may be needed in z-coordinate models before

adding a parameterization of double diffusion can have a demonstrable positive impact on the solutions.

3. Bottom boundary layer and topographic effects

3.1 Bottom friction

Two-dimensional geostrophic turbulence has the property that energy cascades towards large scales, and enstrophy (the relative vorticity squared) cascades towards small scales (Batchelor, 1969). Thus, if eddies have their energy source at a scale close to the internal Rossby radius, nonlinear interactions tend to transfer this energy to larger scales where it must be dissipated. Viscous bottom drag can provide the energy sink which is required to equilibrate the flow. It is thus necessary to include a parameterization of bottom drag in eddy-resolving models. The strength of the bottom drag can have an influence on the spatial organisation of the flow because it affects the baroclinic instability of eastwards jets (Riviere et al., 2004).

Another interesting effect of bottom drag happens in overflow regions. In a rotating fluid, and under the hydrostatic approximation, dense plumes have a strong tendency to follow isobaths rather than plunging. A high bottom friction makes the flow less geostrophic and increases the rate of descent of the plumes (Stratford and Haines, 2000).

Despite such important dynamical effects, there does not seem to be any study documenting the effect of bottom drag in high resolution basin flows, especially in the presence of bottom topography. Most models use a quadratic bottom drag with constant coefficient (Table. 2).

3.2 Effects of overflows

Overflows are currents from marginal or semi-enclosed seas into the main ocean basins, through sills or along continental slopes. They set the properties of many water masses (Price and Yang, 1998). A major difficulty in modelling overflows is that many of them are subgrid scale physics for a given choice of resolution: the width of the strait or channel is narrower than the grid size. Note that straits can be one grid point-wide on a staggered "C" grid such as used in the OPA code, but two grid points are necessary to allow throughflow on a "B" grid with no-slip boundary condition (see Haidvogel and Beckmann, 1999, for a definition of staggered grids). The modeller may decide to open too wide a strait. In that case, the transport may be too large due to the exaggerated cross-section. G. Madec (personal communication) decreases the grid

size locally at a strait: but this trick is possible only when the strait is between land points because the grid size $\delta x, \delta y$ does not depend on z. It cannot be used for deep fracture zones in the middle of ocean basins.

The influence of overflow waters is especially important in the North Atlantic, with North Atlantic Deep water (at depths of 2000-3000 m) coming over Denmark Straits and the Faroe-Scotland ridge, Mediterranean water (1000 m depth) coming through Gibraltar, and Antarctic bottom water (4000 m depth) spreading over sills in the mid-Atlantic ridge (Romanche and Vema fracture zones, for example). The overflows are very badly represented in z coordinate models with staircase topography, generally leading to excessive mixing (Willebrand et al., 2001). There are simple models (such as streamtubes) to calculate exchange between basins in simplified cases, that could be the basis for parameterizations (Price and Yang, 1998). The problem with this method is that each overflow must be specified at a given grid cell or set of grid cells, which is quite cumbersome in a world ocean. Another drawback is that such a parameterization introduces grid scale sources and sinks that may not be handled well by the numerics.

Modellers look for parameterizations valid everywhere in the domain, such as the "Bottom boundary layer" (BBL) parameterization (Beckmann and Döscher, 1997). Since this pioneering work, BBL parameterizations have been implemented in many ocean models. However, we don't have yet a complete picture of their efficiency, depending on model characteristics. Dengg et al. (1999) find that a BBL parameterization induces a large improvement in a 1/3° model of the Atlantic using a centered advection scheme. However in the 1/6°model of the Atlantic we find that the improvement is modest, although the BBL parameterization is similar and both models use the same isopycnal mixing of tracers (Fig. 7). What causes the different performance of the BBL parameterization in those two models is unclear; numerical details may matter.

The FOAM model was developped from the HadCM3 ocean component at 1.8° resolution. In the latter, a variant of a diffusive BBL scheme was implemented that dramatically improved the representation of the Nordic seas overflows (Gordon et al., 2000). In this scheme, when bottom water at a grid cell is denser than the deeper water colums around, the algorithm looks for the level of neutral buoyancy of that bottom water and mixes the dense water into that model level. Lighter water is then moved up in the water column to replace the dense water. The behavior of this scheme in the 1/9° version of FOAM has no yet been evaluated in detail.

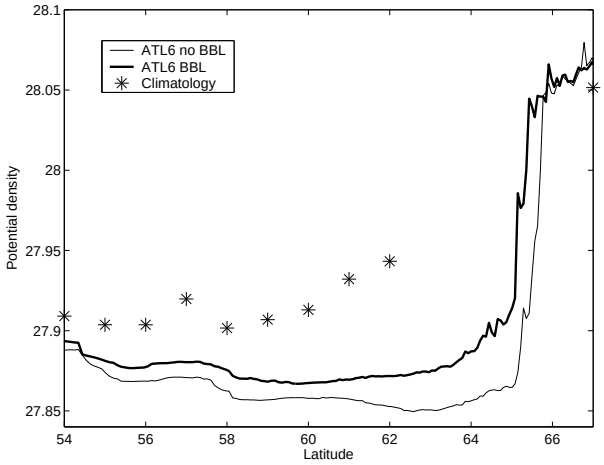

Figure 7. Zonal maximum of bottom density in the Irminger Sea (45°W-25°W), in the climatology and in two ATL6 experiments with and without BBL (the average of the 13rd model year is used).

A new difficulty has appeared with the generalization of the "partial cell" representation of bottom topography in z coordinate models. BBL parameterizations generate fluxes of tracers between bottom cells situated in neighbouring fluid columns. With partial cells the thickness of those bottom cell can vary widely, which may introduce spurious noise in the BBL fluxes.

In this chapter we have chosen examples from z-coordinate models only, but the choice of vertical coordinate is very important for the representation of overflows (Griffies 2005, this book). σ coordinate models handle overflows very well provided their vertical resolution near the bottom is good enough. This was not the case in the DYNAMO σ model, (Willebrand et al., 2001), but one example is the model of the Mediterranean outflow by Jungclaus and Mellor (2000). It is possible in σ models to retain a spatially homogeneous vertical resolution in the bottom boundary layer, which seems ideal for overflow representation, but does have an extra numerical cost.

3.3 Other flow-topography interaction

The interaction of flow with subgrid scale topography can generate internal waves, which can propagate in the water column and increase vertical mixing if they break. This process is generally parameterized as part of the vertical mixing due to internal waves, which has been discussed in section 3.4.

Regarding low frequency motions, the statistical effect of unresolved topographic roughness has been explored in the framework of the quasi-geostrophic (QG) equations, starting with Rhines (1977). The main effect of bottom roughness is to scatter the barotropic energy into baroclinic modes, and decrease the energy of mesoscale motions in the deep layers. There has been no attempt to parameterize this effect in ocean models. On the contrary, the effect of bottom roughness is probably overestimated already in standard z-coordinate models with unsmoothed staircase topography. Penduff et al. (2002) show that in such a model the eddy kinetic energy below 1000 m is lower than in a σ-coordinate model, the latter being in better agreement with observations. By performing sensitivity experiments with the z model they show that the grid-scale topographic roughness is responsible for a too rapid decay of the eddy kinetic energy with depth.

Beside allowing overflows, deep passages and fracture zones often act to sharpen and focus fronts. This effect can influence the whole water column when major currents cross topographic ridges. One example is the flow of the North Atlantic current across the Mid Atlantic ridge, which seems to be distributed in three branches corresponding to three fracture zones (Bower et al., 2002). There is no parameterization of this effect in low resolution models.

4. Lateral mixing parameterizations

4.1 Prandtl number

Let us assume that lateral momentum and tracer mixing are parameterized as laplacian operators with turbulent viscosity ν and diffusivity κ. The ratio of viscosity to diffusivity is the Prandtl number, $Pr = \nu/\kappa$. For molecular viscosity and heat diffusivity in sea water, it varies from 13 (at 0°C) to 7 (at 20°C). Molecular values are irrelevant at the scale of ocean models, and the Prandlt numbers used in models parameterizations vary widely. This is not based on physics but rather the result of numerical stability constraints which seem more stringent on viscosity than diffusivity. In low resolution climate models, Prandtl numbers as high as 50 can be found.

At the scale of quasi-geostrophic eddies, the Prandtl number could be one if one accepts that QG eddies essentially mix potential vorticity. In that case, mixing of vortex stretching (with diffusivity κ) has to be the same as mixing of relative vorticity (with viscosity ν). At the submesoscale, I do not know of theories nor observations that would guide modellers in a choice of Prandtl number.

4.2 Isopycnal mixing of tracers

Let us consider lateral mixing operators in our eddy permitting models (table 2). Some models use a laplacian operator rotated to follow the isopycnal (neutral) direction, others use a horizontal biharmonic (bi-laplacian) operator. The biharmonic operator has been introduced in quasi-geostrophic models based on the properties of two-dimensional turbulence. Because it is more scale-selective, it allows a model to represent a larger part of the mesoscale spectrum at a given grid resolution, while removing variance at the grid scale at a sufficient rate to avoid grid scale noise. However, the biharmonic operator can cause spurious overshoots in tracer properties (Mariotti et al., 1994), so that it has disadvantages as well as advantages. The inconveniences are pointed out in more detail by Griffies (2004).

Examination of the basin-scale water mass properties reveals that they spread along isopycnals (not horizontally), due to advection and stirring by mesoscale eddies. Analysis of tracer release experiments (Ledwell et al., 1998) suggest that mixing is isopycnal down to scales of 100 m, so that there is no evidence to support the choice of a horizontal mixing as in PSY2 or MFS. Toole (1998) reviews the processes that may be responsible for isopycnal mixing at different scales. Shear dispersion due to near-inertial internal waves can cause an isopycnal diffusivity of ≈ 0.07 m^2.s^{-1} at scales between 100 m and 1 km. Vortical modes could be responsible for diffusivities of ≈ 2 m^2.s^{-1} at scales 1 to 30 km, and mesoscale eddies can cause diffusivities up to 1000 m^2.s^{-1} at scales larger than 300 km. The eddy resolving models using isopycnal mixing cannot be run with diffusivities as low as observed; FOAM for example uses $\kappa = 100$ m^2.s^{-1}. This large value is needed to avoid numerical accumulation of enstrophy at the model grid scale (12 km).

¿From the observations of Ledwell et al. (1998), it seems that isopycnal diffusivities increase roughly linearly with the length scale. This would justify the choice made by some modellers to make the diffusivity proportional to the grid scale (or the third power of the grid scale in the case of a biharmonic operator), as for example in the DYNAMO models (Willebrand et al., 2001), or in PSY2.

The above considerations would support the choice of a biharmonic operator (for its scale selectiveness), rotated along isopycnals for consistency with observations. Often though, modellers do not want to pay the computational cost of rotating the biharmonic. This explains why the two alternatives found in table 2 are a horizontal biharmonic and an isopycnal laplacian. Those two parameterizations were compared during the CLIPPER project. Two experiments were run with the ATL6 model,

one using a horizontal biharmonic coefficient (like PSY2 and MFS) with value of 5.5 10^{10}m^4.s^{-1} at the equator, and the other one using a isopycnal laplacian mixing (like FOAM) with coefficient 200 m^2.s^{-1}. Results were not conclusive. The meridional overturning was enhanced by 2 Sv with the isopycnal mixing, which was assumed to be an improvement, but the deep jets analyzed by Treguier et al. (2003) were weaker with isopycnal mixing and the Agulhas eddies seemed too stable.

To make progress with the parameterization of lateral mixing at the sub-mesoscale, we need to understand the physical processes better. Sub-mesoscales are difficult to observe, but high resolution quasi-geostrophic or two-dimensional models give us insights into their behavior. One key phenomenon in the tracer cascade to small scales is the formation of elongated filaments, which occurs preferentially at critical points around the eddies when they interact with each other. This flow structure with energetic eddy cores surrounded by filaments is found in all high resolution models. Fig. 8 shows an example in the PSY2 model without data assimilation). Recent studies help understand where and when filaments form as a function of resolved flow quantities (see for example Klein et al., 2000). Parameterizations based on such analysis in physical space (by opposition to the more usual biharmonic or hyperviscosities based only on the cascade in spectral space) look promising, like the one by Dubos and Babiano (2002). So far they have not been implemented in realistic primitive equation models.

If mixing at the submesoscale is mainly performed by the combined action of vertically sheared inertial oscillations and vertical mixing as proposed by Young et al. (1982), then a parameterization must include the effect of mesoscale eddies on the inertial oscillations. Such a parameterization is tested by Klein et al. (2003) in quasi-geostrophic models and shown to cause an assymetry between anticyclonic and cyclonic structures.

One important issue that is too often ignored in parameterizations of isopycnal mixing is the large inhomogeneity of the mesoscale eddy field, which is now very well mapped from satellite altimetry. Obviously the isopycnal diffusivity κ in non-eddy resolving model should depend on the eddy activity. One possible way to achieve that is to use a scaling based on the time scale for baroclinic instability (Treguier et al., 1997). Such spatially variable coefficients have been used to represent the dynamical effect of eddies (see next section), but their use for mixing of tracers along isopycnals is not documented. Note that sharp variations in the eddy mixing coefficient κ can increase the gradients of tracers along isopycnals, as shown in Fig. 5. It will also create an advection of tracers away from the regions of active eddies. This advection is different

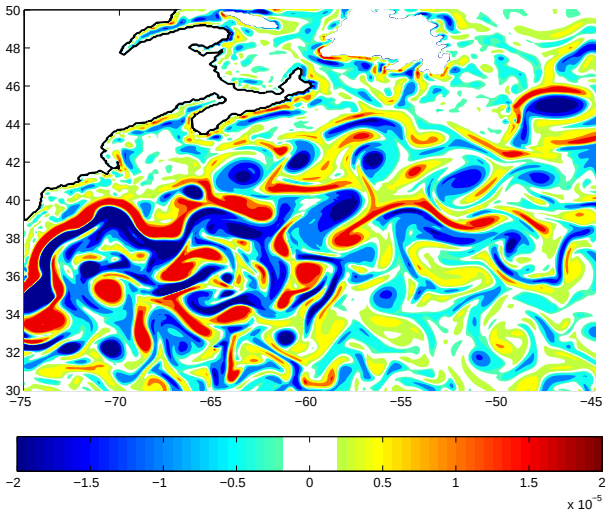

Figure 8. Relative vorticity (in s^{-1})at 17m depth in the PSY2 model without data assimilation (averaged over 5 days).

from the advective effect of the antisymmetric component of the mixing tensor (7), because contrary to V^* the velocity V_κ due to the spatial variation of κ is divergent. Both V^* and V_κ are needed to fully represent the difference between Eulerian and Lagrangian velocities (Plumb and Mahlman, 1987).

Another well known feature of diffusivity due to mesoscale eddies is its anisotropy. Because of the β-effect, mesoscale motions have longer zonal than meridional scales (Rhines, 1977). Ledwell et al. (1998) found a factor of two between the zonal and meridional diffusivity deduced from the spreading of his tracer. Despite this evidence, the use of anisotropic diffusivity in ocean models is not documented.

4.3 Lateral mixing of momentum

There are no observations similar to the tracer releases that would give us insight in the mechanisms of momentum mixing in the ocean, and theories do not help much either. Well known properties of mesoscale eddies, like their tendency to concentrate momentum in an eastward jet on a β plane (McWilliams and Chow, 1981) are very difficult to parameterize because they would involve counter-gradient fluxes.

For lack of physically motivated parameterizations, modellers generally use simple laplacian or biharmonic viscosity operators. The values of the coefficients are subject to two numerical constraints. In basin

scale models, the smallest spatial scale is often the width of the western boundary current. When it is controlled by laplacian friction it is called a Munk boundary layer. The condition that the grid scale δx be smaller than the Munk layer width results in a minimum bound for viscosity (Smith and McWilliams, 2003): $\nu > \nu_M \approx \beta \delta x^3$. On the other hand, viscosity cannot be arbitrarily large due to the stability constraint (similar to the CFL criterion for advection). This criterion is more severe in ocean models that use explicit leap-frog time stepping schemes for nonlinear advection, with the viscous terms lagged by one time step for stability. For laplacian viscosity $\nu < \delta x^2 / 8\,\delta t$. For a biharmonic operator the criterion is $\nu < \delta x^4 / 64\,\delta t$ (biharmonic coded as in the POP model) or $\nu < \delta x^4 / 128\,\delta t$ (biharmonic coded as in the OPA model).

For the laplacian operator on coarse grids, the Munk layer constraint implies very large viscosities: with δx=10 km at 45°N, $\nu_M = 16$ m^2.s^{-1}, but with δx=100 km, $\nu_M = 16000$ m^2.s^{-1}. It is impossible to represent equatorial dynamics with such a large viscosity, which is why this constraint is not always taken into account. For example, in the FOAM 1° model the viscosity is 5100 m^2.s^{-1}. In that case, some level of grid point noise usually develops near the western boundary. A second strategy is to decrease the viscosity at the equator, while increasing the meridional resolution there (parameterization of the ORCA2 model with $\nu = 2000$ m^2.s^{-1} at the equator and $\nu = 40000$ m^2.s^{-1} at mid-latitudes, Madec et al., 1998). Finally, Large et al. (2001) have proposed to make the viscosity anisotropic, noting that the equatorial current are dominantly zonal while Munk boundary currents are predominantly meridional. This solution however does not prevent the apparition of numerical noise.

For the biharmonic operation the numerical stability criterion is often more stringent than the Munk layer constraint. With δx=10 km, the latter gives $\nu > \beta \delta x^5 = 1.6\ 10^9$ m^4.s^{-1}. With a 1200 s time step, numerical stability requires that $\nu < \delta x^4 / 64\,\delta t = 1.3\ 10^{11}$ m^4.s^{-1}. A decrease of the biharmonic coefficient with the grid spacing is often needed in order to ensure stability on spatially variable grids, as in the case of PSY2 (Table 2). Based on numerical experiments with a 1/12° isopycnic model, Chassignet and Garraffo (personal communication) suggest that the Gulf stream separation is improved using together a laplacian and a bilaplacian operator. This has prompted the use of both operators in FOAM (Table 2).

Smagorinsky (1963) has proposed to make the laplacian viscosity proportional to the deformation rate times the squared grid spacing δx^2. Such a parameterization can be physically motivated in three dimensional turbulence and is used in large eddy simulations. In ocean mod-

els it has mainly been used in MICOM (Bleck and Boudra, 1981). A study by Griffies and Hallberg (2003) suggests that using a biharmonic operator with Smagorinsky-like viscosity is better in eddy permitting simulation when the flow is non homogeneous (in the presence of western boundary currents, for instance) because it allows lower levels of viscosity in the interior.

This short review emphasizes numerical constraints as the basis for the choice of parameterizations of momentum mixing. We can hope that more physically based parameterizations will emerge in the future. Smith and McWilliams (2003) have developed a promising framework by deriving a general form for anisotropic viscosity, and an elegant functional form for the discretization following a similar work by Griffies et al. (1998) on the isoneutral diffusion.

For completeness we must mention here another approach to parameterizations. It consists in using the properties of numerical advections schemes to represent the cascade of enstrophy to small scales (this also applies to cascade of tracer variance reviewed in the previous section). With that strategy, no explicit parameterization is needed. Shchepetkin and McWiliams (1998) advocate this approach, claiming that higher Reynolds numbers can be simulated that way, compared with the combination of a classical advection scheme and hyperviscosity. Those authors also claim that it is more computationaly efficient to increase the accuracy of the advection scheme rather than increasing the spatial resolution. This is certainly true for the idealized turbulence experiments they perform, but it is probably not yet true for realistic ocean models. Subgrid scale topographic effects are the reason for this. Refining the grid offers the opportunity to better represent key straits and passages, which a higher order scheme cannot provide. This is certainly the reason why most ocean models still use second order, inexpensive advection schemes. This situation may change in the future, as higher spatial resolutions are allowed by the computational resources.

5. Dynamical effects of mesoscale eddies

5.1 Baroclinic instability

Gent and McWilliams (1990), hereafter GM, have noted that parameterizing the mixing of salinity and temperature anomalies on isopycnals by mesoscale eddies is not enough, because this leaves aside the dynamical effect of eddies on the density field. Most of the eddy energy in the ocean is believed to arise due to baroclinic instability of the mean flow. Baroclinically unstable eddies extract available potential energy from the mean flow, thus tending to flatten isopycnals. The GM parameteriza-

tion proposes that this effect is best represented using the antisymmetric part of the diffusion tensor (5), that is, by an additional advection of the density field. They propose to make this velocity proportional to the isopycnal slope (a pedagogical presentation of their parameterization is found in Gent et al., 1995). This parameterization was the first physically-based original parameterization for coarse resolution ocean model, and as such it has known a rapid success. It certainly improves the climate model solutions especially in the Antarctic circumpolar current, although too large advective velocities for the GM parameterization have negative effects there (Speer et al., 2000).

It is useful to consider the parameterizations in the quasigeostrophic limit (Treguier et al., 1997), in which case GM corresponds to a mixing of potential vorticity (more precisely, the vortex stretching contribution to potential vorticity) along isopycnals. Therefore, the coefficient used for the GM parameterization can be considered as a mixing coefficient for potential vorticity, while the coefficient used for isopycnal mixing is relevant to a passive tracer (temperature and salinity anomalies along isopycnal surfaces). Two-dimensional turbulence emphasizes the similarity between the dynamics of vorticity and passive tracers; although no similar studies exist with primitive equations in three dimensions there is no physical argument to justify widely different mixing coefficients for the two parameterizations. It is thus very surprising to find that many modellers take coefficients for their GM parameterizations that are spatially dependent on the level of baroclinic instability as proposed by Treguier et al. (1997) or Visbeck et al. (1997), thus correctly taking into account the inhomogeneity of the eddy activity in the ocean, while they keep the isopycnal mixing coefficient constant. Maybe modellers are reluctant to seek guidance from the quasi-geostrophic framework because things are indeed more complex in primitive equations: for example, the GM parameterization as usually implemented is closer to a mixing of isopycnal depth than to a mixing of potential vorticity.

A most important open question is how to represent the unresolved part of the mesoscale eddy spectrum in eddy permitting models. First, it is important to note that the unresolved spectrum varies with latitude. A typical spatial scale for baroclinic instability is the first Rossby radius R_1. Even though model grids are often of Mercator type, refined as the cosine of latitude, they still fall short of resolving R_1 in the Labrador Sea and Nordic seas where it can be a few kilometers in winter. Perhaps we should be more precise about what is meant by "resolving". A minimum requirement could be 12 grid points per wavelength (a first derivative estimated with a second order finite difference scheme still has 5% error in that case), thus $\delta x < 2\pi R_1/12 \approx R_1/2$. Chanut (2003)

finds a dramatic improvement in the representation of restratification after convection in the Labrador Sea between a 18 km grid and a 3-4 km grid (1/3° to 1/15°). Certainly, a full GM parameterization would be justified in the 1/3° model, in the Labrador Sea but not elsewhere. The eddy fluxes in Chanut's high resolution case correspond to GM coefficient of up to 800 $m^2.s^{-1}$. If such a high value is used in the subtropical gyre it destroys the eddy activity in the Gulf Stream. The spatially variable form proposed by Visbeck et al. (1997) does not help in that case, because baroclinic instability growth rate is higher in the Gulf Stream than in the Labrador Sea based on the resolved flow field. Studies are under way to propose variants of the GM parameterization that would "switch on" when needed.

Considering a case where the first Rossby radius is well resolved (say, a 5 km grid where $R_1 = 40$ km), how should the dynamical effect of sub-mesoscale eddies be parameterized? Is the unresolved part of the spectrum mainly controlled by baroclinic instability? Roberts and Marshall (1998) advocate the use of a biharmonic GM parameterization, based on their wish to eliminate diapycnal mixing in the surface layers. However, this requirement may not be physically defensible, considering that eddies do perform diapycnal (horizontal) mixing across surface fronts (Treguier et al., 1997). As was the case for in the two previous parameterizations we considered (isopycnal diffusivity and lateral viscosity) we still lack observational evidence and theory to justify parameterizations of the submesoscale effects.

5.2 Other mesoscale eddy effects

Another dynamical effect of mesoscale eddies is the so-called "Neptune" effect (see for a review Alvarez and Tintoré, 1998). In the presence of bathymetry and β-effect, quasigeostrophic eddies have the tendency to generate mean flows along f/H contours. This additional mean flow must be forced by a parameterization when eddies are not represented in a model. The problem is that we do not have enough knowledge of the strength of this effect in realistic ocean circulations and neither do we know the vertical structure of the generated mean flows. Certainly, adding a parameterization forcing barotropic currents along f/H contours would help Atlantic models to improve the strength of their deep western boundary currents. However, if the models do not represent the overflow correctly, the Neptune parameterization could have the effect of generating spurious transport of water with the wrong properties.

Finally, mesoscale eddies tend to exist as coherent structures that carry water far from their generation region (well-known examples are

Meddies and Agulhas eddies). The effects of such eddies are highly non-local, and no parameterization has yet been proposed for such processes.

6. Conclusion

Parameterizations and resolution are the two fundamental characteristics of an ocean model. By choosing them, we actually pick up the "ocean" we try to model. We have reviewed different parameterizations, based on the example of the forecast models listed in tables 1 and 2. What emerges from this review is a rather unsatisfactory state of affairs. Some paramerizations are well grounded in physics (like convection) and have been evaluated by comparison with more complete models (non-hydrostatic in this case). Even then, though, we find that some features are not completely agreed upon among modellers (like the Prandtl number) and modifying them has a strong effect on the solution of low resolution models. But this is the best situation. Generally, the parameterizations do not have sound physical basis, have not been fully evaluated against laboratory experiments or more complete models, and there are strong numerical constraints limiting the choices of modellers.

The boundaries of the ocean, at the bottom and at the surface, are places where progress needs to be made. Regarding the bottom, the main problem is the representation of flow-topography interactions in z-coordinate ocean models. This is an issue of numerics rather than parameterization, which is discussed in the chapter by Griffies. The main effect of staircase topography in z-coordinate models, which is not completely alleviated by using a partial step representation, is the existence of large and noisy vertical velocities which often contaminate the upper layers (especially on the continental slopes). This is a big obstacle to the use of such models for biogeochemistry. Hybrid models like HYCOM may be better candidates for such applications, although it is not clear that numerical factors affecting the communication between the surface z layer and the interior isopcynic layers will not prove an even bigger obstacle. It is quite surprising that although σ coordinate models are extensively used for regional and coastal modelling, no larger scale σ configurations have been built for demonstration purposes, either for climate prediction or forecasting.

The representation of the surface layers in ocean models is perhaps the point where progress is the most likely in the coming years. Today, model solutions in the mixed layer critically depends on the parameterizations. This dependency may decrease as we resolve more physical processes. It is possible to do so with existing parameterizations simply by increasing the vertical resolution (to about 1 m) and using higher

frequency forcing (thus taking into account wind-forced inertial oscillations and the diurnal cycle). Improving the representation of surface layers is critical for operational forecast models because many clients need accurate surface velocities. It is also important in coupled models for climate prediction.

My personal view is that parameterization of the full mesoscale eddy spectrum is a hopeless challenge. We can certainly improve on existing parameterizations. Low-resolution climate models will still be necessary tools in the future, because (fortunately) many aspects of the long-term climate response are robust with respect to details of mesoscale eddy effects. On the other hand, growing computer power will help us to resolve a larger part of the mesocale eddy spectrum in forecast models. It is therefore very important to improve our knowledge of the sub-mesoscale dynamics and develop suitable parameterizations. In this respect, it is quite possible that progress will be easier to achieve in the ocean than in the atmosphere. Atmospheric climate models resolve a large part of the synoptic scale eddies and use crude parameterizations of the subgrid scale dynamics. This is because subgrid scale physics linked to atmospheric moisture (cloud physics, radiation) play a more important role in climate than purely dynamical subgrid scale effects. Ocean models do not have this additional level of complexity and may be a more suitable framework to develop parameterisations for the dynamics, which would fully take into account the spatial inhomogeneity of the mesoscale eddy field.

Acknowledgments

I thank Patrice Klein for useful discussions and for pointing out equation (9). Comments from Steve Griffies and GODAE school students have been very helpful.

References

Alvarez, A. and Tintoré, J. (1998). Topographic stress: importance and parameterization. In *Ocean Modeling and Parameterization*, volume 516 of *NATO Science series C*, pages 327–350. Kluwer Academic Publishers.

Arhan, M., Mercier, H., and Lujtjeharms, J.R.E. (1999). The disparate evolution of three agulhas rings in the south atlantic ocean. *J. Geophys. Res.*, 104:20987–21005.

Batchelor, G. K. (1969). Computation of the energy spectrum in homogeneous two-dimensional turbulence. *Phys. Fluids.*, 12, II:233–238.

Beckmann, A. and Döscher, R. (1997). A method for improved representation of dense water spreading over topography in geopotential-coordinate models. *J. Phys. Oceanogr.*, 27:581–591.

Blanke, B. and Delecluse, P. (1993). Variability of the tropical atlantic ocean simulated by a general circulation model with two different mixed layer physics. *J. Phys. Oceanogr.*, 23:1363–1388.

Bleck, R. and Boudra, D. B. (1981). Initial testing of a numerical circulation model using a hybrid- (quasi-isopycnic) vertical coordinate. *J. Phys. Oceanogr.*, 11:755–770.

Boer, G. J. and Denis, B. (1997). Numerical convergence of a gcm. *Climate dynamics*, 13:359–374.

Bower, A. S., Cann, B. Le, Rossby, T., Zenk, W., Gould, J., Speer, K., Richardson, P. L., Prater, M. D., and Zhang, H. M. (2002). Directly-measured mid-depth circulation in the northeastern north atlantic ocean. *Nature*, 419 (6907):603–607.

Chanut, J. (2003). *Paramétrisation de la restratification après convection profonde en mer du Labrador*. PhD thesis, université Joseph Fourier, Grenoble, France.

Chanut, J. and Molines, J. M. (2004). Implementation et validation du modèle kpp dans opa8.1. Rapport technique, LEGI, Grenoble.

Chassignet, E. and Verron, J., editors (1998). *Ocean Modeling and Parameterization*, volume 516 of *NATO Science series C*. Kluwer Academic Publishers, Cambridge.

Cox, M. D. (1984). A primitive equation, 3-dimensional model of the ocean. Technical Report 1, Geophysical Fluid Dynamics Laboratory, PO Box 308, Princeton, New Jersey, 08542.

Dengg, J., Böning, C., Ernst, U., Redler, R., and Beckmann, A. (1999). Effects of improved model representation of overflow water on the subpolar north atlantic. *WOCE Newsletter*, 37.

Dengler, M., Schott, F., Eden, C., Brandt, P., Fischer, J., and Zantopp, R. J. (2004). New mechanisms for deep water transport. *Nature*. In press.

Dubos, T. and Babiano, A. (2002). Two-dimensional cascades and mixing: a physical space approach. *J. Fluid. Mech.*, 467:81–100.

Gent, P.R. and McWilliams, J.C. (1990). Isopycnal mixing in ocean circulation model. *J. Phys. Oceanogr.*, 20:150–155.

Gent, P.R., Willebrand, J., McDougall, T.J., and McWilliams, J.C. (1995). Parameterizing eddy-induced tracer transports in ocean circulation models. *J. Phys. Oceanogr.*, 25:463–474.

Gerdes, R. (1993). A primitive equation ocean circulation model using a general vertical coordinate transformation. *J. Geophys. Res.*, 98:14683–14701.

Gordon, C., Cooper, C., Senior, C. A., Banks, H., Gregory, J. M., Johns, T. C., Mitchell, J. F. B., and Woods, R. A. (2000). The simulation of sst, sea ice extents and ocean heat transports in a version of the hadley centre coupled model without flux adjustments. *Climate Dynamics*, 16:147–168.

Griffies, S. M. (2004). *Fundamentals of ocean climate models*. Princeton University Press, Princeton, U.S.A.

Griffies, S. M., Boening, C., Bryan, F.O., Chassignet, E. P, Gerdes, R., Hasumi, H., Hirst, A., Treguier, A.M, and Webb, D. (2000a). Developments in ocean climate modelling. *Ocean Modelling*, 2:123–192.

Griffies, S. M., Gnanadesikan, A., Pacanowski, R. C., Larichev, V. D., Dukowicz, J. K., and Smith, R. D. (1998). Isoneutral diffusion in a z-coordinate ocean model. *J. Phys. Oceanogr.*, 28:805–830.

Griffies, S. M. and Hallberg, R. W. (2000). Biharmonic friction with a smagorinsky-like viscosity for use in large scale eddy-permitting ocean models. *Monthly Weather Review*, 128:2935–2946.

Griffies, S. M., Pacanowski, R. C., and Hallberg, R. W. (2000b). Spurious diapycnal mixing associated with advection in a z-coordinate ocean model. *Monthly Weather Review*, 128:538–564.

Haidvogel, D.B. and Beckmann, A. (1999). *Numerical Ocean Circulation Modelling*, volume 2 of *Series on environmental science and management*. Imperial College Press, London.

Hasumi, H. and Suginohara, N. (1999). Effects of locally enhanced vertical diffusivity over rough bathymetry on the world ocean circulation. *J. Geophys. Res.*, 104:23367–23374.

Hurlburt, H. E. and Hogan, P. J. (2000). Impact of 1/8° to 1/64° resolution on gulf stream model-data comparisons in basin-scale subtropical atlantic models. *Dyn. Atmos. Oceans*, 32:283–329.

Jungclaus, J. H. and Mellor, G. (2000). A three-dimensional model study of the mediterranean outflow. *J. Mar. Sys.*, 24:41–66.

Klein, P., Hua, B. L., and Carton, X. (2003). Emergence of cyclonic structures due to the interaction between near-inertial oscillations and mesoscale eddies. *Q. J. R. Meteorol. Soc.*, 129:1–20.

Klein, P., Hua, B. L., and Lapeyre, G. (2000). Alignment of tracer gradients in two-dimensional turbulence using second order lagrangian dynamics. *Physica D*, 146:246–260.

Klinger, B. A., Marshall, J., and Send, U. (1996). Representation of convective plumes by vertical adjustment. *J. Geophys. Res.*, 101:18175–18182.

Kraus, E. B. and Turner, S. (1967). A one-dimensional model of the seasonal thermocline. ii: The general theory and its consequences. *Tellus*, 19:98–106.

Large, W. G. (1998). Modelling and parameterizing the ocean planetary boundary layer. In *Ocean Modeling and Parameterization*, volume 516 of *NATO Science series C*, pages 81–120. Kluwer Academic Publishers.

Large, W. G., Danabasoglu, G., McWilliams, J.C., Gent, P. R., and Bryan, F. O. (2001). Equatorial circulation of a global ocean climate model with anisotropic horizontal viscosity. *J. Phys. Oceanogr.*, 31:518–536.

Large, W.G., McWilliams, J.C., and Doney, S.C. (1994). Oceanic vertical mixing: a review and a model with a nonlocal boundary layer parameterization. *Reviews of Geophysics*, 32:363–403.

Laurent, L. C. St, Simmons, H. L., and Jayne, S. R. (2002). Estimating tidally driven mixing in the deep ocean. *Geophys. Res. Lets*, 29:2106.

Ledwell, J. R., Watson, A. J., and Law, C. S. (1998). Mixing of a tracer in the pycnocline. *J. Geophys. Res.*, 103:21499–21529.

Madec, G., Delecluse, P., Imbard, M., and Levy, C. (1998). Opa 8.1 general circulation model reference manual. Notes de l'ipsl, Univ. Pierre et Marie Curie, Paris.

Maltrud, M. E. and McClean, J. L. (2004). An eddy resolving global 1/10° ocean simulation. *Ocean Modelling*, 7:31–54.

Mariotti, A., Legras, B., and Dritschel, D. G. (1994). Vortex stripping and the erosion of coherent structures in two-dimensional flows. *Phys. Fluids*, 6:3934–3962.

Matteoli, O. (2003). Etude de sensibilité d'orca2 à la physique verticale des couches de surface. Rapport de stage, LODYC, Univ. Pierre et Marie Curie, Paris.

McWilliams, J. C. and Chow, J. (1981). Equilibrium turbulence i: a reference solution in a β-plane channel. *J. Phys. Oceanogr.*, 11:921–949.

Mellor, G. L. and Yamada, T. (1982). Development of a turbulence closure model for geophysical fluid problems. *Rev. Geophys. and Space Phys.*, 20:851–875.

Merryfield, W. J., Holloway, G., and Gargett, A. E. (1999). A global ocean model with double-diffusive mixing. *J. Phys. Oceanogr.*, 29:1124–1142.

Pacanowski, R. C. and Philander, S. G. H. (1981). Parameterization of vertical mixing in numerical models of the tropical ocean. *J. Phys. Oceanogr.*, 11:1442–1451.

Penduff, T., Barnier, B., Verron, J., and Kerbiriou, M. A. (2002). How topographic smoothing contributes to differentiating the eddy flows simulated by sigma- and z-level models. *J. Phys. Oceanogr.*, 32:122–137.

Phillips, O. M. (1972). Turbulence in a strongly stratified fluid - is it unstable? *Deep Sea Res.*, 19:79–81.

Plumb, R. A. and Mahlman, J.D. (1987). The zonally averaged transport characteristics of the gfdl general circulation/transport model. *J. Atmos. Sci.*, 44:298–327.

Price, J. F. and Yang, J. (1998). Marginal sea overflows for climate simulations. In *Ocean Modeling and Parameterization*, volume 516 of *NATO Science series C*, pages 155–170. Kluwer Academic Publishers.

Rhines, P. B. (1977). *The dynamics of unsteady currents*, volume 6 of *Marine Modelling, The Sea*, pages 189–318. Wiley.

Riviere, P., Treguier, A. M., and Klein, P. (2004). Effects of bottom friction on nonlinear equilibration of an oceanic baroclinic jet. *J. Phys. Oceanogr.*, 34:416–432.

Roberts, M. and Marshall, D. (1998). Do we require adiabatic dissipation schemes in eddy-resolving ocean models? *J. Phys. Oceanogr.*, 28:2050–2063.

Ruddick, B. R., McDougall, T. J., and Turner, J. S. (1989). The formation of layers in a uniformly stirred density gradient. *Deep Sea Res.*, 36:597–609.

Schmitt, R. W. (1998). Double-diffusive convection. In *Ocean Modeling and Parameterization*, volume 516 of *NATO Science series C*, pages 215–234. Kluwer Academic Publishers.

Send, U. and Käse, R. H. (1998). Parameterization of processes in deep convection regimes. In *Ocean Modeling and Parameterization*, volume 516 of *NATO Science series C*, pages 191–214. Kluwer Academic Publishers.

Shchepetkin, A. F. and McWilliams, J. C. (1998). Quasi-monotone advection schemes based on explicit locally adaptative dissipation. *Monthly Weather Review*, 126:1541–1580.

Siegel, A., Weiss, J. B., Toomre, J., McWilliams, J. C., Berloff, P. S., and Yavneh, I. (2001). Eddies and vortices in ocean basin dynamics. *Geophys. Res. Lets.*, 28:3183–3186.

Simmons, H. L., Jayne, S. R., Laurent, L. C. St., and Weaver, A. J. (2004). Tidally driven mixing in a numerical model of the ocean general circulation. *Ocean Modelling*, 6:245–263.

Smagorinsky, J. (1963). General circulation experiments with the primitive equations: I. the basic experiment. *Monthly Weather Review*, 91:99–164.

Smith, R. D., Maltrud, M. E., Bryan, F. O., and Hecht, M.W. (2000). Simulation of the north atlantic ocean at $1/10^{\circ}$. *J. Phys. Oceanogr.*, 30:1532–1561.

Smith, R. D. and McWilliams, J. C. (2003). Anisotropic horizontal viscosity for ocean models. *Ocean Modelling*, 5:129–156.

Speer, K., Guilyardi, E., and Madec, G. (2000). Southern ocean transformation in a coupled model with and without eddy mass fluxes. *Tellus*, 52A:554–565.

Stratford, K. and Haines, K (2000). Frictional sinking of the dense water overflow in a z-coordinate ogcm of the mediterranean sea. *Geophys. Res. Lets.*, 27:3973–3976.

Toole, J. M. (1998). Turbulent mixing in the ocean. In *Ocean Modeling and Parameterization*, volume 516 of *NATO Science series C*, pages 171–190. Kluwer Academic Publishers.

Treguier, A. M., Barnier, B., de Miranda, A. P., Molines, J.M., Grima, N., Imbard, M., Messager, C, Reynaud, T, and Michel, S (2001). An eddy permitting model of the atlantic circulation: evaluating open boundary conditions. *J. Geophys. Res.*, 106:22115–22129.

Treguier, A. M., Held, I., and Larichev, V. (1997). On the parameterization of quasi-geostrophic eddies in primitive equation ocean models. *J. Phys. Oceanogr.*, 27:567–580.

Treguier, A. M., Hogg, N. G., Maltrud, M., Speer, K., and Thierry, V. (2003). Origin of deep zonal flows in the brazil basin. *J. Phys. Oceanogr.*, 33:580–599.

Visbeck, M., Marshall, J., Haine, T., and Spall, M. (1997). Specification of eddy transfer coefficients in coarse resolution ocean circulation models. *J. Phys. Oceanogr.*, 27:381–402.

Willebrand, J., Barnier, B., Böning, C., Dieterich, C., Hermann, P., Killworth, P. D., LeProvost, C., Jia, Y., Molines, J. M., and New, A. L. (2001). Circulation characteristics in three eddy-permitting models of the north atlantic. *Prog. Oceanogr.*, 48:123–161.

Young, W. R., Rhines, P. B., and Garrett, C. J. R. (1982). Shear-flow dispersion, internal waves and horizontal mixing in the ocean. *J. Phys. Oceanogr.*, 12:515–527.